Supporting Information

Acid-Responsive Liposomal Nanodrug with Promoted Tumor Penetration for Photoacoustic imaging-guided Sonodynamic Therapy

Xiangli Li[a], Wen-Jing Tang[a], Wei Wang[a], Shuzhen Yue*[a], Huiqin Yao*[b], and Jun-Jie Zhu*[a]
[a] X. Li, W.-J. Tang, W. Wang, S. Yue and J.-J. Zhu
State Key Laboratory of Analytical Chemistry for Life Science, School of Chemistry and Chemical Engineering, Nanjing University, Nanjing 210023, China
[b] H. Yao
Department of Medical Chemistry, College of Basic Medicine, Ningxia Medical University, Yinchuan 750004, China.

Email: jjzhu@nju.edu.cn; shuzhyue@163.com; yaohq@nxmu.edu.cn

Experimental Section

Apparatus and Characterization. Transmission electron microscopy (TEM) images were collected from a JEM-1011 transmission electron microscope (JEOL, Japan). Dynamic light scattering (DLS) characterization was performed on a 90 Plus Nanoparticle Size Analyzer (Brookhaven, USA). Zeta potential analysis was conducted on a Nano-Z zeta potential analyzer (Malvern Instruments, USA). Confocal laser scanning microscopy (CLSM) imaging was conducted using a TCS SP8 confocal laser microscope (Leica, Germany). The ultraviolet-visible (UV/Vis) spectra were collected from the UV-3600 UV/Vis spectrometer (Shimadzu, Japan). Mass spectra were collected from LTQ-Orbitrap X high resolution mass spectrometer (Thermofisher, USA). Electron spin resonance (ESR) spectra were collected from the EMX PLUS (PPMS) paramagnetic resonance spectrometer (Bruker BioSpin, Germany). Flow cytometry analysis was performed on a Beckman Coulter CytoFlex S instrument (Beckman Coulter, USA). *In vitro* and *in vivo* PA imaging was performed on a Vevo LAZR photoacoustic imaging system (Fujifilm, Japan).

Materials and Reagents. 1,2-Dioleoyl-sn-glycero-3-phosphoethanolamine (DOPE) was purchased from Jiangsu Aikang Biopharmaceutical Co., Ltd. (Jiangsu, China). Lys-Boc(Lys)-NHS was purchased from Bidepharm Technology Co., Ltd. (Shanghai, China). Cy5, acetylcholine bromide, 2,3-dimethylmaleic anhydride (DA) and trifluoroacetic acid (TFA) were purchased from Macklin Reagents Co., Ltd. (Shanghai, China). 1,2-Dioleoyl-sn-glycero-3-phosphoethanolamine-polyethylene glycol (DOPE-PEG_{2000}), 2,2-azobis[2-(2-imidazolin-2-yl) propane] dihydrochloride (AIPH), soybean phospholipid (SPC), D-aspartic acid and succinic anhydride (SA) were purchased from Aladdin Reagents Co., Ltd. (Shanghai, China). 2,2'-azino-bis(3-ethylbenzothiazoline-6-sulfonic acid) (ABTS) was purchased from Sigma-Aldrich Co., Ltd. (Shanghai, China). 3-(4,5-dimethylthiazol-2-yl)-2,5-diphenyltetrazolium bromide (MTT) was purchased from KeyGen BioTECH Co., Ltd. (Nanjing, China).

Synthesis of DOPE-Lys-DA and DOPE-Lys-SA. The synthesis route of DOPE-Lys-DA is shown in Figure S1a. Firstly, DOPE (45 mg, 0.06 mmol) and Boc-Lys (Boc)-NHS (39.9 mg, 0.09 mmol) were mixed in CH_2Cl_2, then 20 μL TEA was added to the mixture. After stirring at room temperature for 12 h, the DOPE-Lys-Boc was obtained (**Compound 1**). Following the removal of the solvent, 600 μL of anhydrous CH_2Cl_2 and 95 μL of TFA were mixed with the **Compound 1** under ice bath, and the mixture was stirred for 5 h. After rotary evaporation to remove the solvent, DOPE-Lys (**Compound 2**) was obtained. Then, **Compound 2** was dissolved in methanol, dialyzed for three days using a dialysis bag (MWCO = 500 Da), and finally freeze dried, resulting in a yield of 78.5%. For the synthesis of DOPE-Lys-DA (**Compound 3**), **Compound 2** (1.4 mg) and DA (4 mg) were dissolved in anhydrous DMSO (100 μL). Subsequently, pyridine (100 μL) and TEA (100 μL) were added to the mixture, which was stirred overnight under nitrogen in an ice bath. The product was then dialyzed for three days using a dialysis bag (MWCO=1000 Da) in 1 mM NaOH solution, followed by freeze-drying to obtain **Compound 3**. The synthesis of DOPE-Lys-SA (**Compound 4**) was followed similar procedure as **Compound 3**, with the exception that DOPE-Lys was reacted with SA at a mole ratio of 1: 20 (Figure S1b).

Preparation of AB@D-DA and AB@D-SA liposomal nanodrugs. The AB@D-DA liposomal nanodrug was prepared via thin-film hydration. In detail, the lipid mixture (DOPE-Lys-DA: SPC: DOPE-PEG2000: Cholesterol = 1: 1: 0.1: 0.9, mol: mol) were dissolved in CH3Cl. Following this, the solvent was removed via rotary evaporation, and the resulting mixture was vacuum-dried for 4 h at room temperature. Subsequently, PBS (pH 7.4, 10 mM) containing AIPH (5 mg/mL) and ABTS (2.5 mg/mL)

was added for hydration. The sample was then sonicated using a cell disruptor (20 W) for 1 min, yielding AB@D-DA. The preparation process for AB@D-SA was identical to that of AB@D-DA, with the exception of replacing DOPE-Lys-DA in the formulation with DOPE-Lys-SA.

The encapsulation efficiency of AIPH and ABTS. To determine the encapsulation efficiency of AIPH and ABTS in AB@D-DA or AB@D-SA liposomal nanodrugs, the standard curves depicting the variation of MS signals for AIPH and ABTS with respect to their concentrations were constructed using Nano-DESI mass spectrometry. A series of AIPH or ABTS solutions were prepared at varying concentrations (2 μg/mL, 5 μg/mL, 10 μg/mL, 15 μg/mL, 20 μg/mL) in a solvent mixture of water and methanol (1:1, v/v). Prior to MS analysis, 5 μM of acetylcholine bromide was added to the AIPH solutions as an internal standard, and the analysis was conducted in positive ion mode. For ABTS, D-aspartic acid (5 μg/mL) was introduced as an internal standard under negative ion mode during MS analysis.

Dialysates from AB@D-DA and AB@D-SA liposomal nanodrugs were collected and diluted with water to a final volume of 50 mL for subsequent use. Before MS injection, 5 μM of acetylcholine bromide was added to the dialysate as an internal standard to quantify the relative signals of AIPH in positive ion mode. D-aspartic acid (5 μg/mL) served as the internal standard for ABTS quantification in negative ion mode. Utilizing the established standard curves, the concentrations of AIPH or ABTS in the dialysates were calculated, thereby enabling the computation of their respective encapsulation efficiency within the liposomal nanodrugs.

Preparation of Cy5-labelled AB@D-DA, Cy5-labelled AB@D-SA and Cy5-labelled AB@D-L. Firstly, DOPE-Lys (1.3 mg), Cy5 (1.0 mg), EDC·HCl (0.88 mg), HOBT (0.62 mg) and DIPEA (5 μL) were dissolved in DMSO (300 μL) and stirred overnight. Subsequently, the resulting product was then purified by dialysis in methanol using a dialysis bag (MWCO = 1000 Da) for 3 days. Following this, the Cy5-labelled DOPE-Lys was obtained through freeze-drying.

Then, the Cy5-labelled AB@D-DA (Cy5-AB@D-DA) was prepared via thin-film hydration. The formulation (DOPE-Lys-DA: SPC: DOPE-PEG_{2000}: Cy5-labelled DOPE-Lys: Cholesterol = 1: 1: 0.1: 0.01: 0.9, mol: mol) were dissolved in CH_3Cl (450 μL). Following this, the solvent was removed via rotary evaporation, and the resulting mixture was vacuum-dried for 4 h at room temperature. Subsequently, PBS (pH 7.4, 10 mM) containing AIPH (5 mg/mL) and ABTS (2.5 mg/mL) was added for hydration. The sample was then sonicated using a cell disruptor (20 W) for 1 min, yielding Cy5-labelled AB@D-DA.

The preparation process for Cy5-labelled AB@D-SA (Cy5-AB@D-SA) and Cy5-labelled AB@D-L (Cy5-AB@D-L) was identical to that of Cy5-AB@D-DA, with the exception of replacing DOPE-Lys-DA in the formulation with DOPE-Lys-SA and DOPE-Lys, respectively.

Acid-responsive charge conversion of AB@D-DA and AB@D-SA. The acid-responsive charge conversion of AB@D- DA was verified through zeta potential analysis. Briefly, AB@D-DA or AB@D-SA liposomal nanodrugs were dispersed in PBS at pH 7.4 or pH 6.8, and incubated at 37 °C. The zeta potential of the samples was measured at predetermined time points.

The acid responsiveness of DOPE-Lys-DA and DOPE-Lys-SA molecules. DOPE-Lys-DA molecules were dispersed in PBS (pH 7.4 or pH 6.8) and then incubated at 37°C for 4 h. As a control, DOPE-Lys-SA molecules underwent identical experimental condition. The molecular weight was precisely determined using mass spectrometry.

Electron spin resonance (ESR) analysis. For ESR analysis, the radical trapping agent DMPO (20 mM) was added to AB@D-DA suspension (500 μg/mL), and then the samples were treated with US (1.0 W/cm^2) for different times (0 min, 1 min, 3 min, 5 min, 6 min). The samples were then immediately

transferred to a quartz capillary tube, and the ESR spectra were acquired from the EMX PLUS (PPMS) paramagnetic resonance spectrometer.

***In vitro* PA imaging.** Following the treatment of the mixture of AB@D-DA suspension (500 μg/mL) with US for varying durations (0 min, 1 min, 3 min, 5 min, 6 min), PA imaging of each sample was conducted.

Cell culture. The 4T1 and L02 cells were purchased from the Cell Bank of Type Culture Collection of Chinese Academy of Sciences (Shanghai, China). Both cell lines were cultured in DMEM medium containing 10% fetal bovine serum, penicillin (80 U/mL) and streptomycin (0.08 mg/mL) in the cell incubator containing 5% CO_2 at 37 °C.

The cellular uptake capacity of Cy5-AB@D-DA and Cy5-AB@D-SA. The cellular uptake capacity of the liposomal nanodrugs was evaluated by CLSM and flow cytometry, respectively. For CLSM assay, 4T1 cells were treated with Cy5-AB@D-DA at pH 7.4 or pH 6.8 for 4 h, followed by rinsing with PBS. The CLSM images were collected with the excitation of 650 nm. For flow cytometry, 4T1 cells were treated with Cy5-AB@D-DA at pH 7.4 or pH 6.8 for 4 h. Then the cells were harvested and washed with PBS. Finally, the cells were analyzed using the flow cytometer. As a control, 4T1 cells were treated with Cy5-AB@D-SA at pH 7.4 or pH 6.8 for 4 h, followed by CLSM imaging and flow analysis.

The penetration of liposomal nanodrug in 3D tumor spheroid models. 4T1 cells were seeded in an ultralow adhesion 96-well microplate (Corning 7007) at a cell density of 2500 cells per well, and the tumor spheres with a diameter of ~500 μm were formed within one week. To assess the penetration depth of liposomal nanodrugs, the tumor spheres were subjected to various treatments: Cy5-labelled AB@D-DA (Cy5-AB@D-DA) in culture medium (pH 7.4); Cy5-AB@D-DA in culture medium (pH 6.8); Cy5-labelled AB@D-SA (Cy5-AB@D-SA) in culture medium (pH 7.4); Cy5-AB@D-SA in culture medium (pH 6.8); Cy5-labelled AB@D-L (Cy5-AB@D-L) in culture medium (pH 7.4); Cy5-labelled AB@D-L (Cy5-AB@D-L) in culture medium (pH 6.8). Following incubation for 24 h, the tumor spheres were washed with PBS and scanned in Z-axis direction by CLSM with a layer scanning interval of 10 μm.

Intracellular alkyl radical generation. 4T1 cells (1×10^4, 100 μL) were seeded in 4-well plates for 24 h, and then incubated with different samples for 2 h: I: PBS; II: US; III: AIPH; IV: AIPH + US; V: AB@D-SA + US; VI: AB@D-DA + US. The amount of AIPH in all samples was equal (20 μg/mL). After washing the cells with PBS, DCFH-DA (8 μM) was added to the wells and incubated for another 30 min. The cells were then washed with PBS, and the corresponding groups were treated with US (1.0 W/cm^2, 2 min), followed by CLSM imaging. I: PBS; II: US; III: AIPH; IV: AIPH + US; V: AB@D-SA + US; VI: AB@D-DA + US. The amount of AIPH in all samples was equal (20 μg/mL).

***In vitro* cytotoxicity assay.** The biocompatibility of the liposomal nanocarriers was evaluated using MTT assays. L02 cells (8×10^3, 100 μL) were seeded in 96-well plates and cultured for 24 h, followed by incubation with varying concentrations of D-DA or D-SA liposomal nanocarriers for 48 h. After incubation, the medium was replaced with 100 μL of MTT solution (0.5 mg/mL) and further incubated for 4 h. Subsequently, the supernatant medium was discarded, and 100 μL DMSO was added to each well. Cell viability was calculated by measuring the absorbance at 492 nm using a microplate reader.

To evaluate the cytotoxicity of different formulations, 4T1 cells (8×10^3, 100 μL) were seeded in 96-well plates and cultured for 24 h. The cells were then incubated with varying concentrations of AIPH, AB@D-DA or AB@D-SA under pH 6.8 condition for 4 h. Following incubation, US was applied to the cells at 1.0 W/cm^2 for 2 min, and the cells were further cultured for 24 h. Finally, cell viability was determined using the MTT assay as the above-mentioned procedures.

To assess cell survival under US exposure, 4T1 cells (8×10^3, 100 μL) were seeded in 96-well plates

for 24 h. The cells were then exposed to US (1.0 W/cm²) for different time (0 min, 1 min, 2 min, 3 min, 4 min) and further cultured for 48 h. After that, the cell viability was calculated using the MTT assay.

Furthermore, the cytotoxicity of different formulations on 3D tumor spheroid model was evaluated. Tumor spheroids were incubated with varying concentrations of AIPH, AB@D-DA or AB@D-SA under pH 6.8 conditions for 4 h, followed by US treatment at 1.0 W/cm² for 2 min. After an additional 24 h of incubation, the tumor spheroids were washed with PBS and the reacted with CCK-8 (100 μL) for 4 h. Finally, the absorbance at 450 nm was measured to calculate cell viability.

Animal model. The female BALB/c nude mice, aged 4 to 6 weeks, were procured from Hangzhou Ziyuan Biotechnology Co., Ltd. All animal experiments were conducted under the authorization granted by the Jiangsu Animal Care and Use Committee (SYXK(Su) 2021-0034). The animal housing and experimental procedures adhered strictly to the protocols sanctioned by the Animal Ethical and Welfare Committee of Nanjing University, ensuring compliance with the Regulations for the Administration of Affairs Concerning Experimental Animals as stipulated by the Chinese government.

In vivo PA imaging. The mice were injected with AB@D-DA (20 mg/kg) and AB@D-SA (20 mg/kg) liposomal nanodrugs through the tail vein, respectively. After 12 h of administration, PA images of tumor tissue was first acquired as the blank group. Then, the tumor tissues were subjected to US treatment (1.0 W/cm²) for 5 min, followed by PA imaging at specific time points (5 min, 20 min, 30 min, 60 min and 120 min).

In vivo therapy. 4T1 cells (1×10^6, 100 μL) was inoculated on the right dorsal region of mice, and the tumor size reached 75~100 mm^3 within one week. Subsequently, the 4T1 tumor-bearing mice were randomly divided into six groups (n = 4) and injected with various formulations containing an equal amount of AIPH (2 mg/kg) via tail vein: G1: PBS; G2: US; G3: AB@D-SA; G4: AB@D-DA; G5: AB@D-SA + US; G6: AB@D-DA + US. After 12 h injection, US irradiation (1.0 W/cm^2, 5 min) was applied to the tumor area of G5 and G6. The same treatment protocol was repeated on the third and fifth days. During 14 days, body weight and tumor size were recorded every other day, and the tumor size was calculated using the formula: V (mm^3) = Length (mm) × Width $(mm)^2$ / 2. After the treatment period, the mice were euthanized, and tumor tissues were excised for photography, weighing, and further analysis.

To assess lung metastasis, the lungs of mice in each group were harvested at the end of therapy. They were then fixed in Bouin's solution for 12 h, photographed, and the number of lung nodules was quantified for analysis.

Hematoxylin and eosin (H&E) and terminal deoxynucleotidyl transferase dUTP nick end labeling (TUNEL) assay. For H&E staining, tissues underwent an initial fixation process in formalin, subsequently embedded in paraffin. Following this, the tissues were stained utilizing an H&E staining kit (Servicebio, Wuhan, China), and the tissue sections were then visualized under the Nikon DS-U3 optical microscope for detail analysis. In the case of TUNEL apoptosis staining, pre-fixed tumor sections were subjected to staining with the in-situ cell death detection kit (Servicebio, Wuhan, China). Then, the prepared tumor sections were imaged and analyzed under the Nikon DS-U3 optical microscope.

Statistical analysis. All data were presented as mean ± standard deviation (s.d.). To assess the statistical significance of differences, one-way ANOVA with a Tukey posthoc test was employed. All analytical procedures were conducted utilizing Origin software (Origin 2021). Statistical significance was indicated as follows: ***$P < 0.001$, **$P < 0.01$, and *$P < 0.05$. The n.s. represented no significant difference.

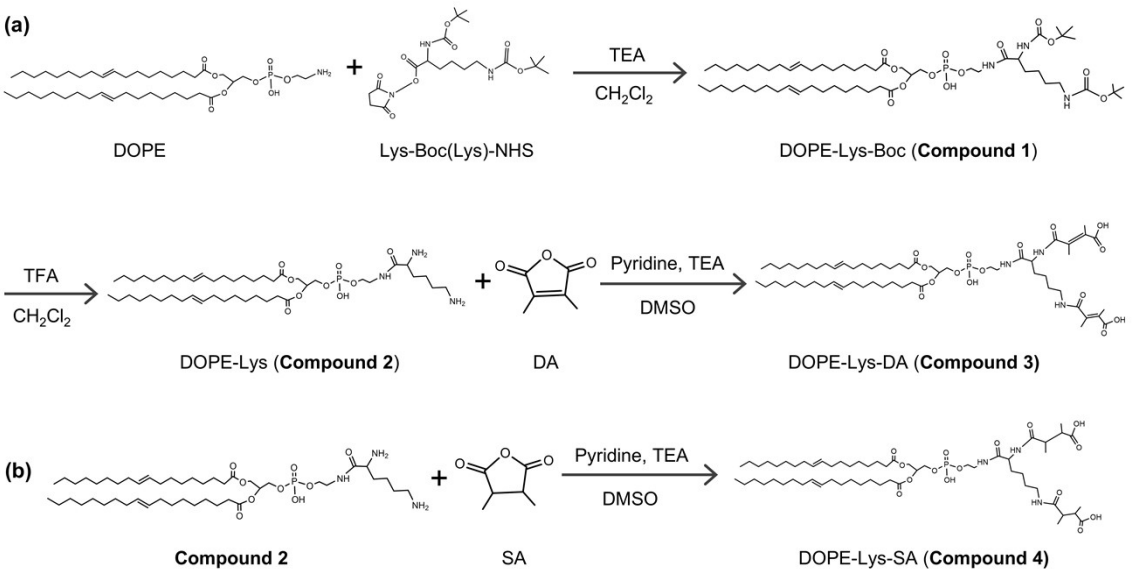

Fig. S1 The synthesis routes of (a) DOPE-Lys-DA and (b) DOPE-Lys-SA molecules.

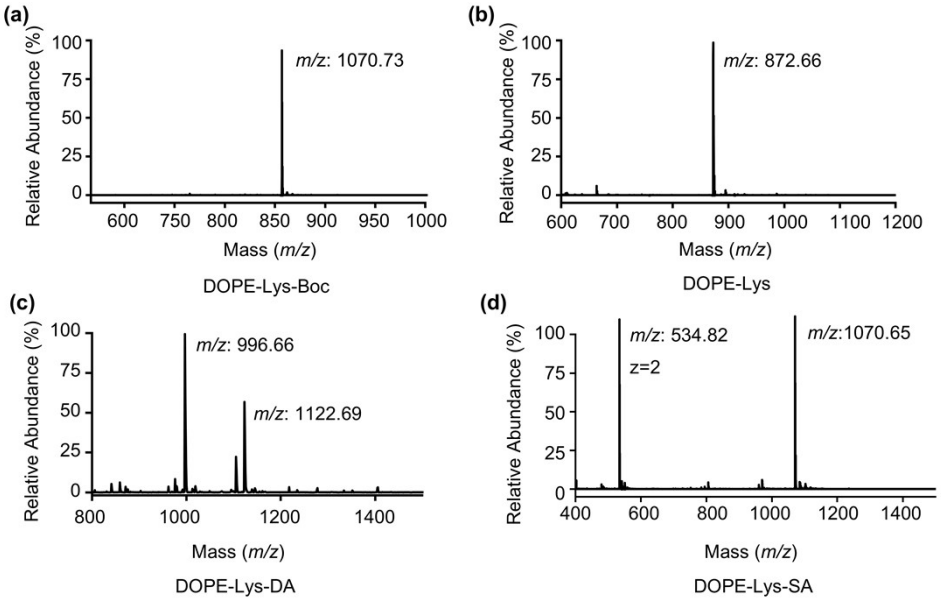

Fig. S2 The mass spectra of (a) DOPE-Lys-Boc, (b) DOPE-Lys, (c) DOPE-Lys-DA and (d) DOPE-Lys-SA molecules.

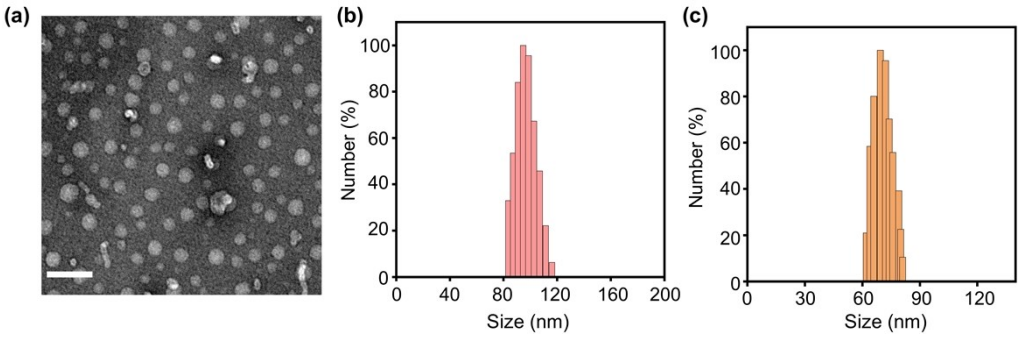

Fig. S3 (a) TEM image of AB@D-SA liposomal nanodrug. Scale bar: 200 nm. Hydrodynamic diameter of (b) AB@D-DA and (c) AB@D-SA liposomal nanodrug.

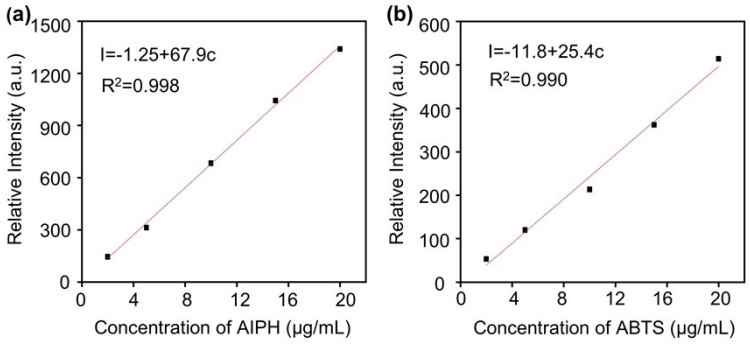

Fig. S4 The calibration curve of relative signal intensity and concentration of (a) AIPH and (b) ABTS in MS analysis. The encapsulation efficiency of AIPH and ABTS within the AB@D-SA liposomes was calculated as 7.7% and 5.5%, respectively.

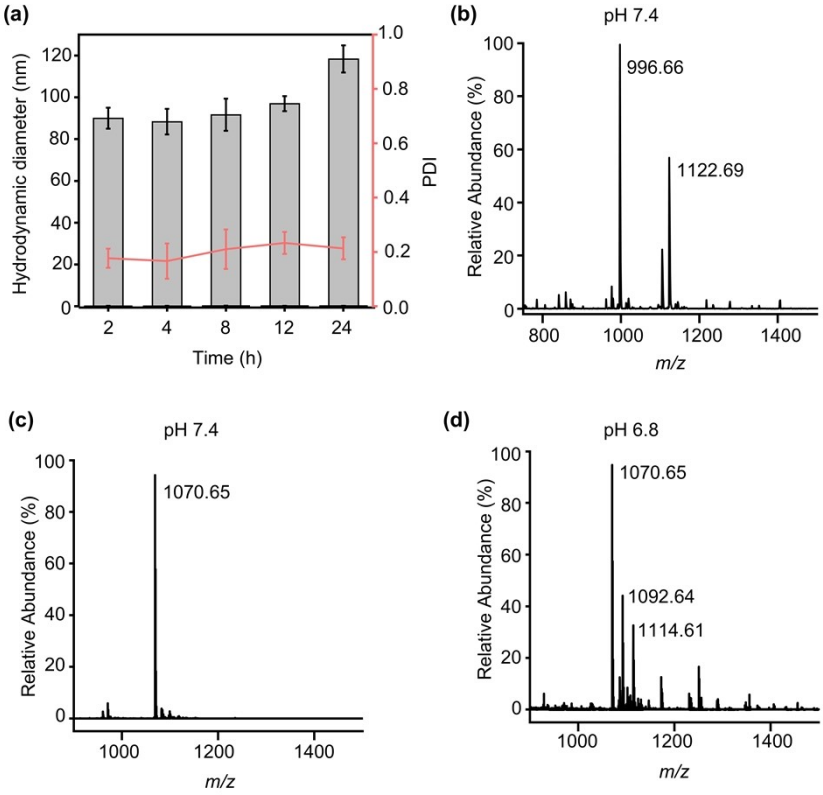

Fig. S5 (a) Hydrodynamic diameter and polydispersity index (PDI) of AB@D-DA under pH 6.8 within 24 h. Error bars represent s.d. (n = 3). (b) The mass spectra of DOPE-Lys-DA molecules in pH 7.4. The mass spectra of DOPE-Lys-SA molecules in (c) pH 7.4 and (d) pH 6.8. *m/z* 1070, *m/z* 1092.64 and *m/z* 1114.61 represent the MS signal of DOPE-Lys-SA, DOPE-Lys-SA + Na^+ and DOPE-Lys-SA + $2Na^+$, respectively.

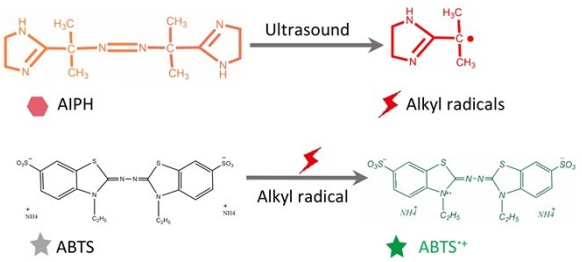

Fig. S6 Scheme illustration of the molecular mechanism of US triggering the generation of alkyl radical and the conversion of ABTS to $ABTS^{\bullet+}$.

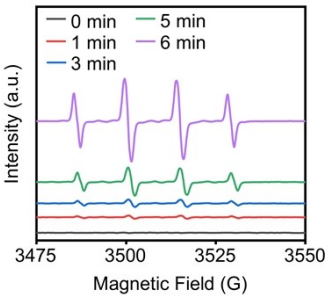

Fig. S7 EPR spectra of the AB@D-DA after US (1.0 W/cm^2) irradiation for different time.

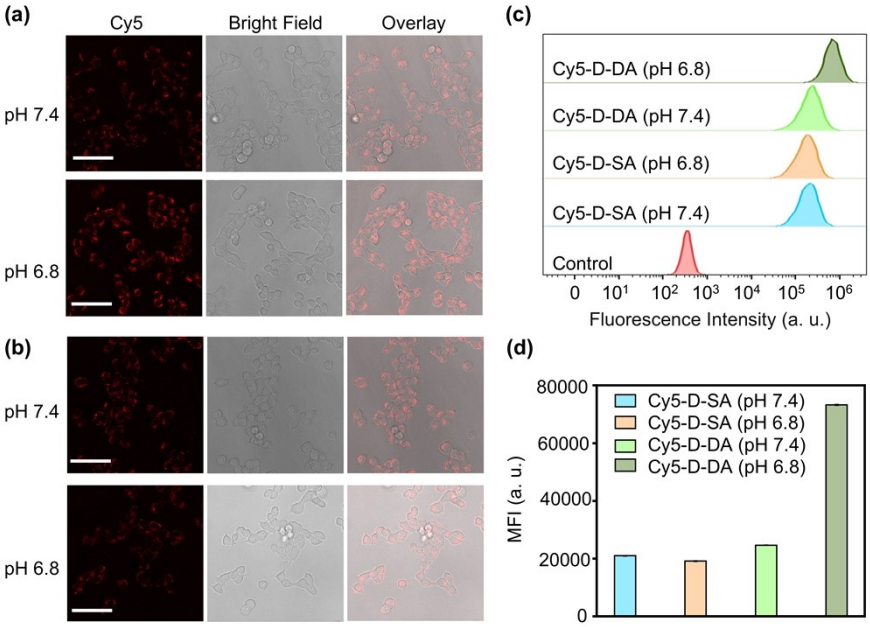

Fig. S8 CLSM images of 4T1 cells treated with (a) AB@D-DA and (b) AB@D-SA under different incubation condition. Scale bar: 75 μm. (c) Flow cytometric analysis and (d) mean fluorescence intensity (MFI) of 4T1 cells after different treatments. Error bars represent s.d. (n = 3).

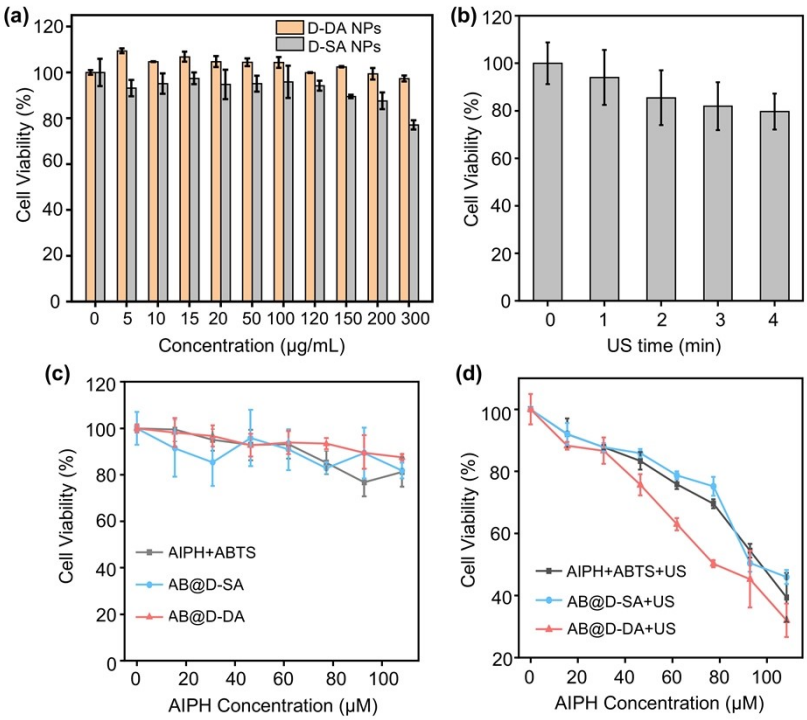

Fig. S9 (a) The cell viability of L02 cells treated with varying concentrations of liposome nanocarriers. (b) The cell viability of 4T1 cells after treatment with US (1.0 W/cm²) for different time. (c) The cell viability of 4T1 cells after different treatments with varying concentrations of AIPH. (d) The cell viability of 4T1 cells after different treatments with varying concentrations of AIPH under US irradiation (1.0 W/cm², 2 min). Error bars represent s.d. (n = 3).

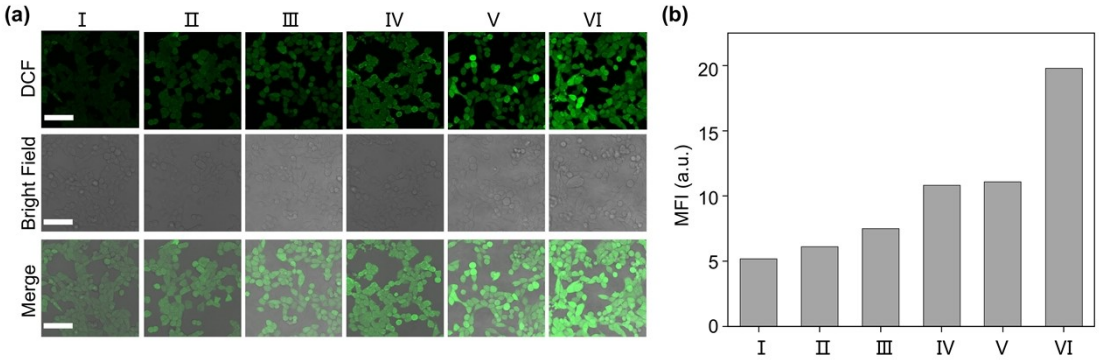

Fig. S10 (a) The CLSM images and (b) mean fluorescence intensity (MFI) of 4T1 cell after different treatments. Scale bar: 75 μm. I: PBS; II: US; III: A + B; IV: A +B + US; V: AB@D-SA + US; VI: AB@D-DA + US.

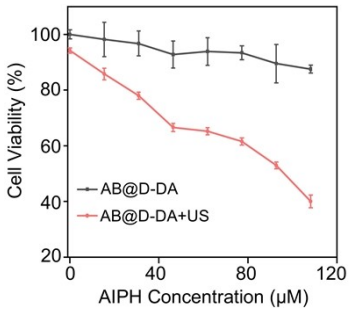

Fig. S11 The cell viability of tumor spheres after treated with varying concentrations of AB@D-DA with or without US (1.0 W/cm², 2 min). Error bars represent s.d. (n = 3).

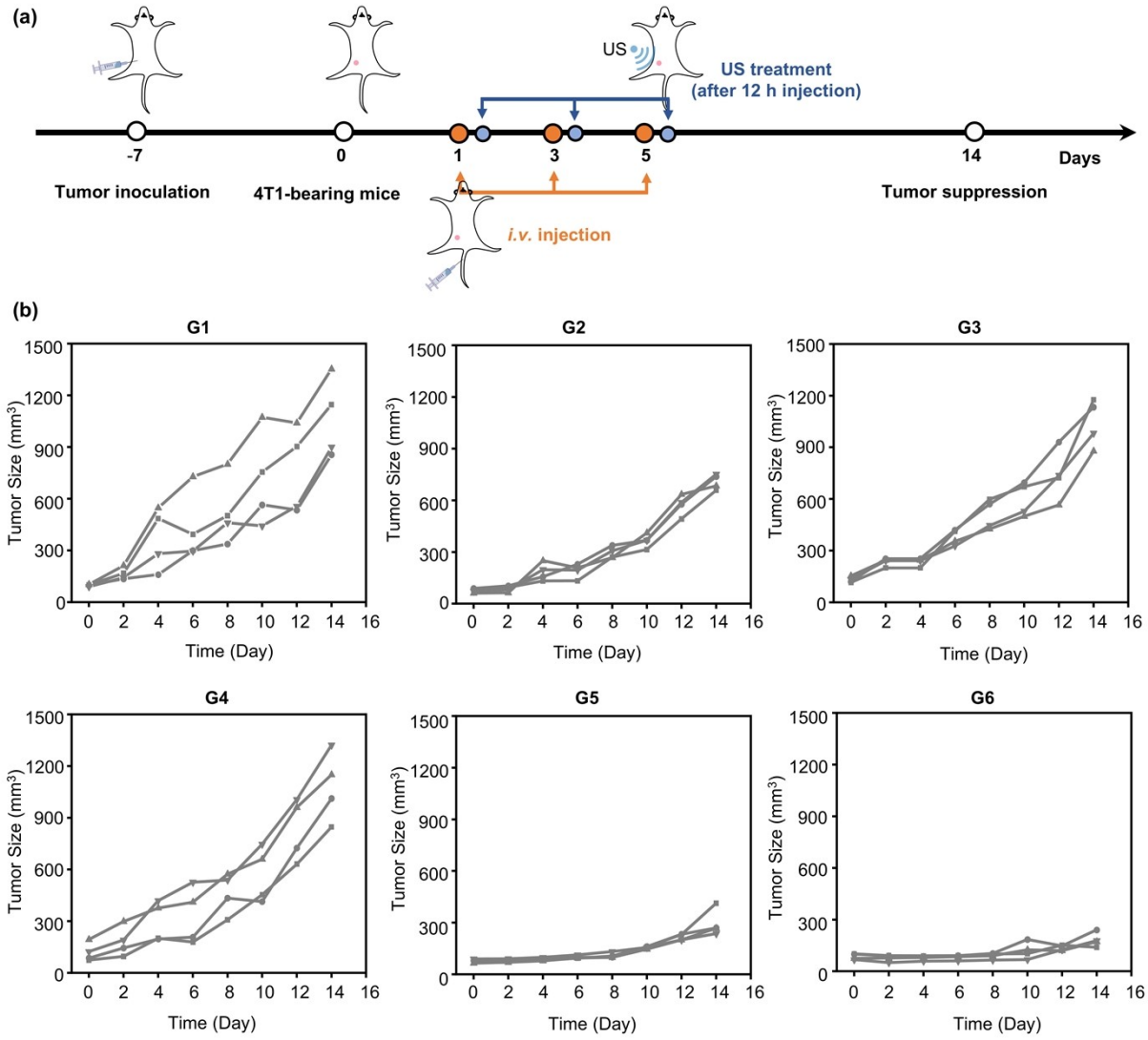

Fig. S12 (a) Scheme illustration of tumor inoculation and SDT. (b) Tumor growth curves of mice in each group. G1: PBS; G2: US only; G3: A + B; G4: A + B + US; G5: AB@D-SA + US; G6: AB@D-DA + US.

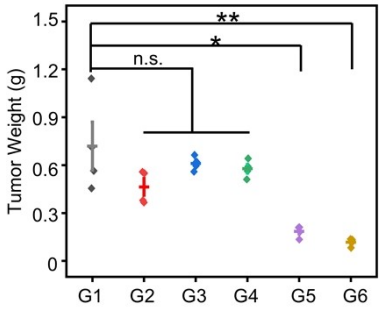

Fig. S13 Tumor weight of harvested tumor tissues at the end of therapy. G1: PBS; G2: US only; G3: A + B; G4: A + B + US; G5: AB@D-SA + US; G6: AB@D-DA + US. Error bars represent s.d. (n = 4).

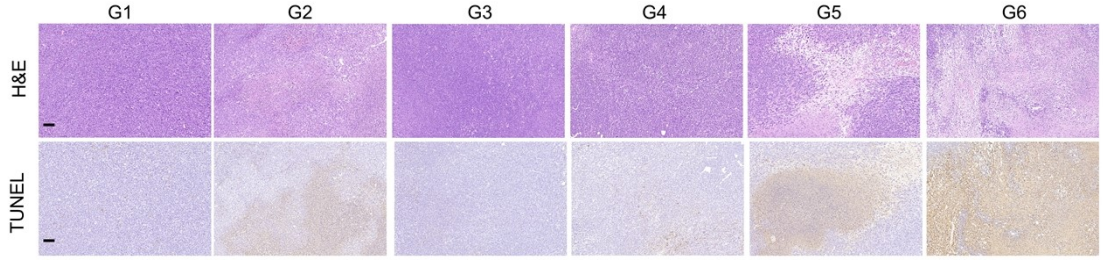

Fig. S14 H&E and TUNEL analysis for tumor tissues at the end of treatment. Scale bar: 100 μm.

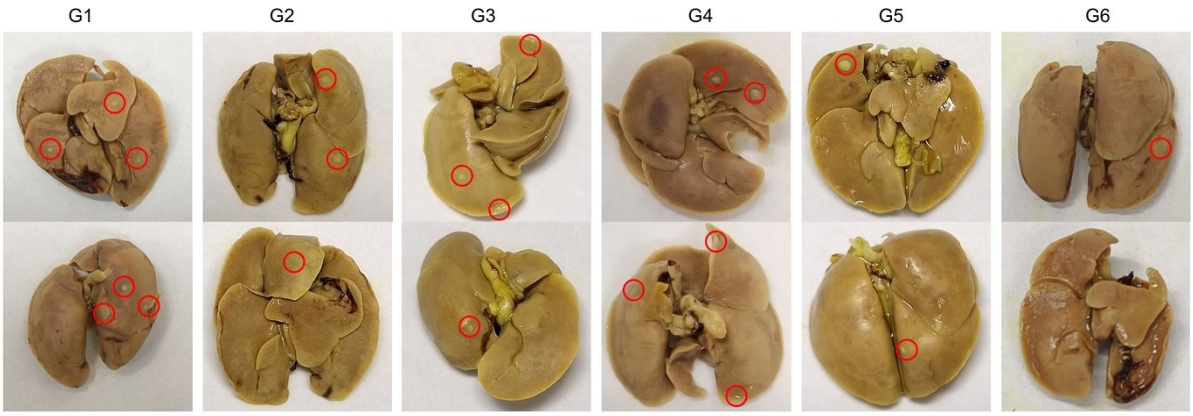

Fig. S15 Photographs of lung tissues, and red circles marked the lung nodules.

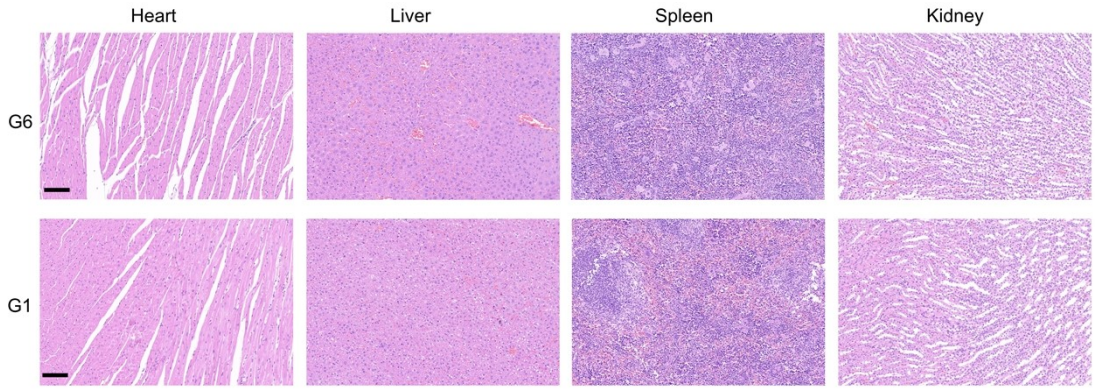

Fig. S16 H&E staning images of major organs in G1 and G6 groups. G1: PBS; G6: AB@D-DA + US. Scale bar: 100 μm.

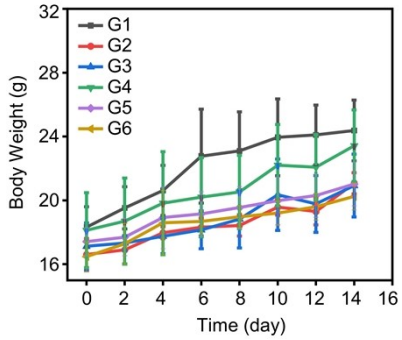

Fig. S17 Average body weight change of each group during the treatment process. G1: PBS; G2: US only; G3: A + B; G4: A + B + US; G5: AB@D-SA + US; G6: AB@D-DA + US. Error bars represent s.d. (n = 4).

Table S1. The IC_{50} values of AIPH in different samples against 4T1 cells.

Samples	IC50 (μM)
A + B	97.72
AB@D-SA	95.50
AB@D-DA	77.62